

meinschaft, the Fonds der Chemischen Industrie, the Technische Universität München, and Degussa for their support.

Registry No. 1, 102149-59-7; **1a**, 102210-45-7; **2**, 102149-62-2; **3**, 102149-65-5; **4**, 101181-55-9; *trans*-[Pt(NH₃)₂(1-MeC)₂]Cl₂, 102210-44-6; *trans*-Pt(NH₃)₂Cl₂, 14913-33-8; *trans*-[Pt(NH₃)₂(1-MeC)₂]-

(NO₃)₂, 76068-67-2.

Supplementary Material Available: Listings of observed and calculated structure factors, atomic parameters, and structural details (64 pages). Ordering information is given on any current masthead page.

Synthesis and Reactivity of the Bridging Thiocarbonyl Radical, Cp₂Fe₂(CO)₂(μ-CO)(μ-CSMe)[•]

Norman C. Schroeder and Robert J. Angelici*

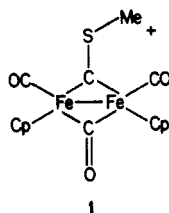
Contribution from the Department of Chemistry, Iowa State University, Ames, Iowa 50011.
Received October 10, 1985

Abstract: The bridging thiocarbonyl radical, Cp₂Fe₂(CO)₂(μ-CO)(μ-CSMe)[•] (**2**), is prepared by a 1-electron reduction of the thiocarbonyl cation, Cp₂Fe₂(CO)₂(μ-CO)(μ-CSMe)⁺ (**1**), with sodium naphthalene or electrochemically (*E*^o = -0.78 V vs. Ag/AgCl). The emerald green radical, **2**, which is sufficiently stable to be studied for an hour at 0 °C, has been characterized by its IR, UV-vis, and EPR spectra as well as its reactions with PhSSPh and PhSeSePh, which give Cp₂Fe₂(EPh)(CO)(μ-CO)(μ-CSMe) and Cp₂Fe₂(CO)₂(μ-CO)[μ-C(SMe)EPh], where E = S or Se. Both the terminal and bridging CO groups of the radical, **2**, exchange rapidly with ¹³CO at 0 °C; this contrasts with cation, **1**, which is inert under these conditions. The lability of the CO groups in **2** makes it a catalyst for the substitution of CO groups by PET₃, PMe₂Ph, PMePh₂, and *t*-BuNC in **1** to form Cp₂Fe₂(L)(CO)(μ-CO)(μ-CSMe)⁺. Cyclic voltammetric studies of **1** in the presence of L suggest that **2** catalyzes these substitution reactions by a radical chain electron transfer mechanism.

Dinuclear transition-metal complexes containing a bridging carbonyl ligand



are well-known,¹ and several reactions which occur at the carbonyl carbon have been described.^{1,2} Recently, we reported³ the reaction of Co(CO)₄⁻ with the bridging thiocarbonyl complex



to give an unusual triply bridging thiocarbonyl complex, Cp₂Fe₂Co(CO)₃(μ-CO)₂(μ₃-CSMe). We noticed^{3,4} that reactions

with relatively strongly reducing metal carbonyl anions (CpFe(CO)₂⁻, Re(CO)₅⁻, and Mn(CO)₅⁻) gave products which could be attributed to processes involving electron transfer from the anion to the thiocarbonyl cation, **1**. In this paper, we report the 1-electron reduction of **1** to give the first example of a bridging dinuclear carbonyl radical, Cp₂Fe₂(CO)₂(μ-CO)(μ-CSMe)[•] (**2**), which has been characterized by its EPR, IR, and electrochemical properties. Radical **2** has also been identified as a key labile intermediate in the catalysis of CO substitution in **1** by chemical and electrochemical reducing agents.

Experimental Section

Unless stated otherwise, all manipulations were carried out under argon or deoxygenated nitrogen in Schlenkware at room temperature. Tetrahydrofuran (THF) was distilled from sodium/benzophenone. Acetonitrile, CH₂Cl₂, and hexane were stirred overnight with CaH₂ and then distilled under N₂. The complex [Cp₂Fe₂(CO)₂(μ-CO)(μ-CSMe)]PF₆ (**1**) was prepared by using a modification⁴ of the method described by Quick and Angelici.⁵ Solutions of sodium naphthalene (NaNp) were prepared by stirring 1:1 molar ratios of sodium and naphthalene in THF.⁶ The salt, NBu₄PF₆ (Bu = *n*-Bu), was prepared by a published procedure.⁷ The phosphines, PET₃, PMe₂Ph, and PMePh₂, were fractionally distilled and stored under N₂. A 1-L flask of 92 atom % ¹³CO was obtained from U.S. Services, Inc., Summit, NJ. All other reagents were commercial products of the highest purity available and were used as received.

A Perkin-Elmer Model 320 or Beckman DU-8 spectrometer was used for measuring UV-visible spectra. Infrared spectra were recorded with a Perkin-Elmer 681 spectrometer. The IR spectra were referenced to the 1603.0-cm⁻¹ band of polystyrene. The ¹H and ¹³C NMR spectra were recorded on a JEOL FX-90Q or Nicolet NT-300 spectrometer and were taken in deuterated (>95.5%) solvents. Chemical shifts were reported in ppm downfield from the internal standard Me₄Si. Electron paramagnetic resonance (EPR) spectra were obtained on samples in CH₃CN (0.1 M NBu₄PF₆) or THF in a 60.0 × 17.0 × 0.25 mm flat quartz cell with a Bruker Model ER 2000-SRC spectrometer. Temperature control

(1) Schroeder, N. C.; Angelici, R. J. *Organometallics*, to be submitted for publication.

(2) For example: (a) Kao, S. C.; Lu, P. P. Y.; Pettit, R. *Organometallics* **1982**, *1*, 911. (b) Dawkins, G. M.; Green, M.; Jeffery, J. C.; Sambale, C.; Stone, F. G. A. *J. Chem. Soc., Dalton Trans.* **1983**, 499. (c) Colborn, R. E.; Davies, D. L.; Dyke, A. F.; Endesfelder, A.; Knox, S. A. R.; Orpen, A. G.; Plaas, D. J. *J. Chem. Soc., Dalton Trans.* **1983**, 2661. (d) Awang, M. R.; Jeffery, J. C.; Stone, F. G. A. *J. Chem. Soc., Dalton Trans.* **1983**, 2091. (e) Casey, C. P.; Marder, S. R.; Fagan, P. J. *J. Am. Chem. Soc.* **1983**, *105*, 7197. (f) Howard, J. A. K.; Jeffery, J. C.; Laguna, M.; Navarro, R.; Stone, F. G. A. *J. Chem. Soc., Dalton Trans.* **1981**, 751. (g) Mead, K. A.; Moore, I.; Stone, F. G. A.; Woodward, P. J. *J. Chem. Soc., Dalton Trans.* **1983**, 2083. (h) Chetcuti, M. J.; Howard, J. A. K.; Millis, R. M.; Stone, F. G. A.; Woodward, P. J. *J. Chem. Soc., Dalton Trans.* **1982**, 1757. (i) Green, M.; Jeffery, J. C.; Porter, S. J.; Razay, H.; Stone, F. G. A. *J. Chem. Soc., Dalton Trans.* **1982**, 2475. (j) Awang, M. R.; Jeffery, J. C.; Stone, F. G. A. *J. Chem. Soc., Chem. Commun.* **1983**, 1426. (k) Barr, R. D.; Green, M.; Howard, J. A. K.; Marder, T. B.; Moore, I.; Stone, F. G. A. *J. Chem. Soc., Dalton Trans.* **1983**, 746. (l) Casey, C. P.; Fagan, P. J. *J. Am. Chem. Soc.* **1982**, *104*, 7360. (m) Ros, J.; Commenges, G.; Mathieu, R.; Solans, X.; Font-Altaba, M. *J. Chem. Soc., Dalton Trans.* **1985**, 1087.

(3) Schroeder, N. C.; Richardson, J. W.; Wang, S. L.; Jacobson, R. A.; Angelici, R. J. *Organometallics* **1985**, *4*, 1126.

(4) Schroeder, N. C. Ph.D. Dissertation, Iowa State University, Ames, Iowa, 1985.

(5) Quick, M. H.; Angelici, R. J. *Inorg. Chem.* **1981**, *20*, 1123.

(6) Paul, D. E.; Lipkin, D.; Weissman, S. I. *J. Am. Chem. Soc.* **1956**, *78*, 116.

(7) Lind, J. E., Jr.; Abdel-Rahim, H. A. A.; Rudich, S. W. *J. Phys. Chem.* **1966**, *70*, 3610.

for EPR measurements was provided by a Bruker ER-4111 variable-temperature controller. Spectra were referenced to diphenylpicrylhydrazide which has a g value of 2.0037 ± 0.0002 .⁸

Cyclic voltammograms were obtained with a Bioanalytical System CV-1B cyclic voltammograph in a conventional three-electrode cell at 0 °C. The working electrode was a platinum disk (3.1 mm²) used in a stationary mode. The reference electrode was Ag/AgCl (3.0 M NaCl); the auxiliary electrode was a platinum wire. Measurements were made in CH_3CN (0.1 M NBu_4PF_6). All solutions were deoxygenated with argon and maintained under an argon atmosphere throughout the measurements.

Electrochemical Preparation of $\text{Cp}_2\text{Fe}_2(\text{CO})_2(\mu\text{-CSMe})^+$ (2). Controlled potential, electrochemical preparations of radical $\text{Cp}_2\text{Fe}_2(\text{CO})_2(\mu\text{-CO})(\mu\text{-CSMe})^+$ (2) were performed with a PAR Model 173 potentiostat/galvanostat with a PAR Model 178 high impedance voltage follower to minimize the length of the connection to the reference electrode for low noise pickup. Experiments were conducted in a three-compartment cell, the compartments being separated by medium porosity frits. A Pt gauze (42 mesh, 2.0×5.0 cm cylinder) was the working electrode. The Ag/AgCl (3.0 M NaCl) reference electrode was separated from the analyte solution by placing it inside a 10 mm i.d. tube with a medium glass frit at the bottom; this tube contained 10 mL of deoxygenated CH_3CN (0.1 M NBu_4PF_6). The auxiliary electrode was a coil of 20 gauge copper wire. A typical preparation of radical 2 was performed as follows: CH_3CN (0.1 M NBu_4PF_6) was added to each cell compartment (30 mL to the sample compartment, 10 mL to the auxiliary compartment, and to the top in the middle compartment) and deoxygenated. After being cooled to 0 °C, the electrolyte solution was pre-electrolyzed at -0.8 V until the current decreased to ca. 0.2 μA . The potentiostatic circuit was disconnected from the working electrode, and $[\text{Cp}_2\text{Fe}_2(\text{CO})_2(\mu\text{-CO})(\mu\text{-CSMe})]\text{PF}_6$ (1) (0.053 g, 0.10 mmol) was added to the sample compartment; the solution in this compartment was deoxygenated and then electrolyzed at -0.8 V under an argon atmosphere at 0 °C with stirring. After 15 min, >90% conversion to radical 2 had occurred (as determined by the intensity of the $\nu(\text{CO})$ bands of 2 or the current used) and the electrolysis was stopped. Solutions of the emerald green radical $\text{Cp}_2\text{Fe}_2(\text{CO})_2(\mu\text{-CO})(\mu\text{-CSMe})^+$ (2) were air-sensitive and thermally unstable; maintained at 0 °C, they slowly turned brown over a 1-h period, and at -80 °C the frozen radical solution turned completely brown after approximately 24 h.

Coulometric determination of the number of electrons (n) involved in the reduction of cation 1 to radical 2 was performed with a PAR Model 179 digital coulometer interfaced with a PAR Model 173 potentiostat/galvanostat. The cell, electrodes, concentrations, and experimental conditions for the coulometric experiments were the same as in the electrochemical preparation of radical 2 described above. The n values were corrected for background current with use of a blank consisting of CH_3CN (0.1 M NBu_4PF_6).

Preparation of $\text{Cp}_2\text{Fe}_2(\text{CO})_2(\mu\text{-CO})(\mu\text{-CSMe})^+$ (2) by Chemical Reduction. By using an air-tight syringe, a THF solution of NaNp (ca. 0.19 mmol/mL) was titrated into a THF (10 mL) suspension of the cation 1 (0.25 g, 0.47 mmol) at 0 °C until solid 2 had completely disappeared. Since 1 is relatively insoluble in THF, this addition was made dropwise with vigorous stirring to prevent further reduction of the radical product. A THF solution of the radical 2 at -80 °C turns brown over a period of 10 h.

^{13}CO Exchange with Radical 2. A THF suspension (10 mL) of cation 1 (0.023 g, 0.043 mmol) was frozen in liquid nitrogen under vacuum and then exposed to a ^{13}CO atmosphere (190 Torr, ca. 0.2 mmol). The frozen suspension was rapidly warmed in a water bath to 25 °C and then vigorously stirred with a magnetic stirring bar for 15 min. IR analysis of the solution showed bands for cation 1 at 2052 (s), 2010 (w), and 1855 (m) cm^{-1} ; no bands for a ^{13}CO exchanged product of cation 1 were observed.

The solution was purged with nitrogen, cooled to 0 °C, and titrated with NaNp (ca. 0.05 mmol/mL in THF) as described above to form the radical. After being frozen with liquid nitrogen under vacuum, the solution was exposed to ^{13}CO atmosphere (190 torr, ca. 0.2 mmol), rapidly warmed in an ice-water bath to 0 °C, and then vigorously stirred for 15 min. The radical was oxidized to cation 1 with I_2 (0.007 g, 0.03 mmol), and the solution taken to dryness; the resulting residue was washed with hexane (20 mL) and extracted with benzene (10 mL). The extract was evaporated to dryness, and the resulting residue was washed with Et_2O (10 mL) and dried. The IR analysis of the residue showed bands for both cation 1 (CH_3CN : 2044 (s), 1853 (m) cm^{-1}) and its ^{13}CO -exchanged product (CH_3CN : 1994 (s), 1811 (m) cm^{-1}). The product is >95% thiocarbonyl cation as indicated by the ^1H NMR spectrum (CD_3CN : δ 5.42 and 5.38 (Cp), 3.60 (Me)). The ^{13}C NMR

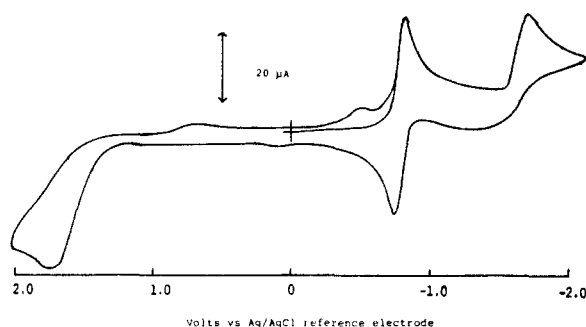


Figure 1. Cyclic voltammogram of $[\text{Cp}_2\text{Fe}_2(\text{CO})_2(\mu\text{-CO})(\mu\text{-CSMe})]\text{PF}_6$ (1) in CH_3CN (0.1 M NBu_4PF_6) at a Pt electrode at 0 °C with a 300-mV/s scan rate.

spectrum (CD_3CN) shows greatly enhanced resonances for the bridging and terminal CO ligands of the thiocarbonyl cation at δ 252.0 and 207.3 (1:2 intensity ratio) as compared with the Cp (δ 92.8 and 92.1) and Me (δ 38.2) peaks.

Reaction of Radical 2 with PhSSPh. Addition of PhSSPh (0.051 g, 0.24 mmol) to the chemically generated radical 2 (0.47 mmol) in THF at 0 °C gave an immediate reaction forming a purple-brown reaction mixture. The solvent was removed under vacuum, and the resulting residue was extracted with hexane to remove naphthalene and the minor coproduct, $\text{Cp}_2\text{Fe}_2(\text{CO})_2(\mu\text{-CO})(\mu\text{-C(SMe)SPh})$.¹ The remaining residue was extracted with 10 mL of CH_2Cl_2 ; the solution was filtered through Celite, concentrated to 4 mL, and layered with hexane (20 mL). Crystallization at -20 °C gave 0.080 g (35%) of brownish-black crystals of $\text{Cp}_2\text{Fe}_2(\text{SPh})(\text{CO})(\mu\text{-CO})(\mu\text{-CSMe})$ (6) with IR (CH_2Cl_2 : 1988 (s), 1809 (s) cm^{-1}) and ^1H NMR spectra (CDCl_3 : δ 7.26 (m, Ph), 4.84 and 4.80 (Cp), 3.39 (Me)) in agreement with values reported¹ for this compound; dp 95 °C.

Reaction of Radical 2 with PhSeSePh. Diphenyldiselenide, PhSeSePh (0.035 g, 0.11 mmol), was added to the chemically generated radical 2 (0.19 mmol) in THF at -80 °C. Warming the reaction to -20 °C gave a purple solution of $\text{Cp}_2\text{Fe}_2(\text{CO})_2(\mu\text{-CO})(\mu\text{-C(SMe)SePh})$ (4) as the only product; it was identified by its IR spectrum (THF: 1982 (s), 1952 (m), 1790 (s) cm^{-1}).¹ However, it is known¹ to be unstable with respect to 5, which was isolated as follows. The purple solution was warmed to room temperature, and the solvent was removed under vacuum. The residue was washed with hexane and extracted with CH_2Cl_2 (20 mL). The extract was filtered through Celite, concentrated at -20 °C, giving 0.030 g (31%) of brownish-black crystals of $\text{Cp}_2\text{Fe}_2(\text{SePh})(\text{CO})(\mu\text{-CO})(\mu\text{-CSMe})$ (5) whose IR (CH_3CN : 1978 (s), 1800 (s) cm^{-1}), ^1H NMR (CDCl_3 : δ 7.32 (m, Ph), 4.84 and 4.75 (Cp), 3.39 (Me)), and ^{13}C NMR spectra (CD_2Cl_2 : δ 403.3 ($\mu\text{-C}$), 261.3 ($\mu\text{-CO}$), 212.9 (CO); 135.3, 134.3, 127.1 and 124.2 (Ph); 88.9 and 87.0 (Cp), 32.8 (Me)) were the same as those reported¹ elsewhere for this compound; dp 95 °C.

Electrocatalytic Preparation of Phosphine and Isocyanide Derivatives, $[\text{Cp}_2\text{Fe}_2(\text{L})(\text{CO})(\mu\text{-CO})(\mu\text{-CSMe})]\text{PF}_6$. Carbon monoxide substitution reactions of cation 1 by PET_3 , PMePh_2 , PMe_2Ph , PPh_3 , and $t\text{-BuNC}$, catalyzed by electrogenerated radical 2, were performed with the cell and apparatus used for the coulometric experiments described above. A typical procedure is reported in detail for the PET_3 case; reactions of the other ligands were performed under the same conditions. A 20.0-mL aliquot of a 3.0×10^{-3} M solution of cation 1 in CH_3CN (0.1 M NBu_4PF_6) was placed in the sample compartment of the electrolysis cell and deoxygenated with argon at 0 °C for 20 min. After adding PET_3 (0.018 mL, 0.12 mmol), the solution was stirred at 0 °C under an argon atmosphere for 1 h. IR analysis of the reaction mixture at this point verified that no reaction had occurred. The solution was then pre-electrolyzed, with stirring, under argon at -0.525 V. When the cathodic current had decreased to <20 μA , the coulometer was reset and the solution was reduced at a controlled current of 1 mA until the potential reached -0.8 V (ca. 150–180 s), when the current was stopped and the coulometer reading was taken. IR analysis of the final reaction mixture only shows $\nu(\text{CO})$ absorptions for $\text{Cp}_2\text{Fe}_2(\text{PET}_3)(\text{CO})(\mu\text{-CO})(\mu\text{-CSMe})^+$ (1987 (s) and 1818 (s) cm^{-1}).⁵ Similar results were obtained for PMePh_2 , PMe_2Ph , and $t\text{-BuNC}$; the PPh_3 reaction was incomplete even after 20 min. An absorbance vs. concentration curve for 1 in CH_3CN (0.1 M NBu_4PF_6) was used to determine the residual concentration of the thiocarbonyl radical in the PPh_3 reaction. These results are summarized in Table I.

Results and Discussion

Cyclic Voltammogram of $[\text{Cp}_2\text{Fe}_2(\text{CO})_2(\mu\text{-CO})(\mu\text{-CSMe})]\text{PF}_6$ (1) Coulometry and Synthesis of $\text{Cp}_2\text{Fe}_2(\text{CO})_2(\mu\text{-CO})(\mu\text{-CSMe})^+$ (2). The cyclic voltammogram of $[\text{Cp}_2\text{Fe}_2(\text{CO})_2(\mu\text{-CO})(\mu\text{-CSMe})]\text{PF}_6$ (1), shown in Figure 1, has two reduction waves with

(8) Drago, R. S. *Physical Methods in Chemistry*; W. B. Saunders Co.: Philadelphia, PA, 1977; p 324.

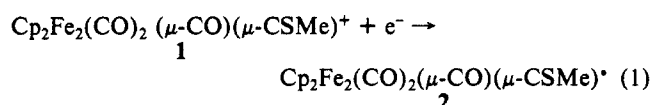
Table I. CO Substitution Reactions (eq 3) of **1**^a Electrocatalyzed by **2** at 0 °C

ligand ^b	product IR ^c	reduction potential (V)	time ^e (s)	coulombs ^e	current efficiency ^f
PEt ₃	1987 (s), 1818 (s)	-1.12	180	0.1825	32.1
PMePh ₂	2005 (s), 1811 (s)	-1.10	146	0.1466	46.1
PMe ₂ Ph	1993 (s), 1814 (s)	-1.14 ^d	150	0.1443	40.8
PPh ₃	2010 (s), 1810 (s) ^g	-1.02	>20 min.	1.728	2.38 ^h
<i>t</i> -BuNC	2010 (s), 1837 (s)	-1.12	165	0.1591	36.9
blank			<5	0.0023	

^a 0.060 mmol of **1** in 20 mL of CH₃CN (0.1 M NBu₄PF₆). ^b 2 equiv. ^c Product infrared bands agree with those reported in ref 4 and 5. ^d Cyclic voltammogram of an authentic sample of [Cp₂Fe₂(PMe₂Ph)(CO)(μ-CO)(μ-CSMe)]⁺ had a reduction potential of -1.14 V reversible. ^e Time and number of coulombs needed to reach a potential of -0.80 V at constant current of 1 mA. ^f Current efficiency = m/n = moles (m) of **1** consumed per faraday of charge (n) passed through the cell. ^g Other products present plus unreacted **1**. ^h Value corrected for the 0.0174 mmol of unreacted **1**.

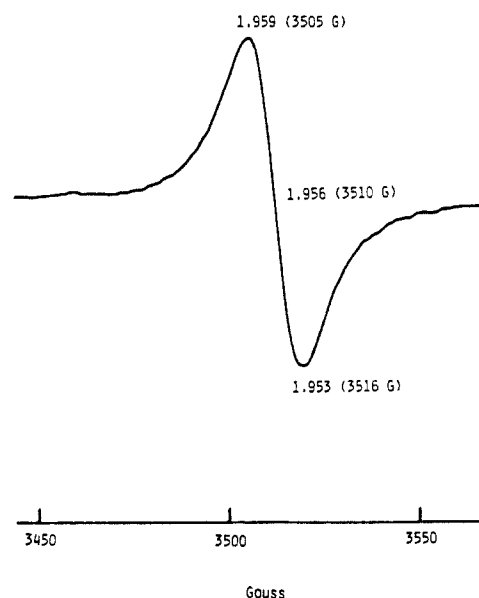
cathodic peak potentials (E_p^c) of -0.82 and -1.70 V. The anodic portion of the irreversible second reduction wave interferes with the first reduction wave. A scan between the voltage limits, 0 to -1.50 V (Figure 3a), eliminates this interference and shows an apparent reversible process for the first reduction step; the ratio of anodic to cathodic peak currents (i_p^c/i_p^a) is near unity. However, the peak-to-peak separation, 75 mV, is greater than predicted for a reversible one-electron reaction. The following results show that this wave is, in fact, quasireversible:⁹ (1) there is little, if any, change in the reduction potential ($E^\circ = (E_p^c + E_p^a)/2 = -0.78$ V vs. Ag/AgCl) with scan rate (v); (2) ($E_p^c - E_p^a$) decreases from 83 mV at $v = 500$ mV/s to 59 mV at $v = 50$ mV/s; and (3) the $i_p^c/v^{1/2}$ ratio is constant.

Controlled potential coulometry at a Pt electrode at -0.8 V vs. Ag/AgCl in CH₃CN (0.1 M NBu₄PF₆) under argon at 0 °C gives an " n " value of 1.00 ± 0.06 electrons. Thus, the electrochemical data indicate that the electrode process at the first reduction wave is



During the course of the electrolysis, the color of the solution changes from brownish-orange to a deep emerald green, indicative of radical Cp₂Fe₂(CO)₂(μ-CO)(μ-CSMe)[•] (**2**). In CH₃CN (0.1 M NBu₄PF₆) at 0 °C, the emerald-green color slowly fades to brown after an hour. The radical decomposes to numerous products, one of which was identified as Cp₂Fe₂(CO)₂(μ-CO)-[μ-C(H)SMe].¹ At -80 °C, the frozen radical solution decomposes over a 24-h period. Chemical reduction of **1** in THF at 0 °C with sodium naphthalene gives the same green color obtained by electrolytic reduction. In this solvent the radical decomposes over a 10-h period at -80 °C. Freshly prepared solutions of **2** are oxidized instantly back to cation **1** upon treatment with I₂. Isolation of Cp₂Fe₂(CO)₂(μ-CO)(μ-CSMe)[•] as a solid was not possible; on concentrating, the THF-radical solution turns brown. The resulting residue after evaporation of THF contains numerous products and does not give [Cp₂Fe₂(CO)₂(μ-CO)(μ-CSMe)]⁺ on reoxidation with I₂.

Spectroscopic Properties. The IR spectrum of Cp₂Fe₂(CO)₂(μ-CO)(μ-CSMe)[•] (**2**) in CH₃CN (0.1 M NBu₄PF₆) has ν(CO) bands at 1973 (s), 1933 (m), and 1760 (m) cm⁻¹. The presence of 2 terminal and 1 bridging band suggests that **2** has a structure similar to that of **1**. The positions of the bands of **2** are 70–90 cm⁻¹ lower than those of the thiocarbonyl cation, **1** (CH₃CN: 2044 (s), 2013 (w), 1853 (m) cm⁻¹). The differences in band positions are expected for the addition of an electron to **1** and are similar to those observed between the μ-carbene complex Cp₂Fe₂(CO)₂(μ-CO)[μ-C(H)SMe]¹ (CH₃CN: 1977 (s), 1938 (w), 1780 (m), cm⁻¹) and [Cp₂Fe₂(CO)₂(μ-CO)(μ-CSMe)]PF₆ (**1**). The IR spectrum of the chemically generated radical (THF: 1978 (s), 1944 (m), 1772 (m) cm⁻¹) has a ν(CO) band pattern similar to that in CH₃CN (0.1 M NBu₄PF₆) except that the

**Figure 2.** EPR spectrum of Cp₂Fe(CO)₂(μ-CO)(μ-CSMe)[•] (**2**) in THF at 183 K.

absorptions occur at slightly higher energy. The relative CO band intensities and their invariance with solvent polarity indicate that **2** probably has a structure in which the Cp groups are cis to each other, as in **1**.⁵

The UV-visible spectrum of Cp₂Fe₂(CO)₂(μ-CO)(μ-CSMe)[•] (**2**) in CH₃CN (0.1 M NBu₄PF₆) has a low-energy band at 602 nm ($\epsilon = 588 \pm 6$ M⁻¹ cm⁻¹) which is red shifted from the low-energy band of [Cp₂Fe₂(CO)₂(μ-CO)(μ-CSMe)]PF₆ (**1**) (500 nm; $\epsilon = 666 \pm 6$ M⁻¹ cm⁻¹) in CH₃CN (0.1 M NBu₄PF₆). The bands in both complexes overlap a much stronger ($\epsilon > 15000$ M⁻¹ cm⁻¹) near-UV band. These spectra are similar to those of other dinuclear metal-metal bonded complexes, such as Cp₂Fe₂(CO)₂(μ-CO)₂ and Cp(CO)₃WCo(CO)₄, which have a low-intensity band ($\epsilon = 500\text{--}700$ M⁻¹ cm⁻¹) at 300–400 nm.¹⁰

The EPR spectrum (Figure 2) of **2** taken in THF at 183 K gives a singlet with a " g " value of 1.956 ± 0.002 . No hyperfine coupling to the protons on either the Cp rings or the methyl group is observed. Molecular orbital calculations^{2c} on bridging carbyne cations indicate that the LUMO is composed mainly of the out-of-plane " p " orbital located on the carbyne carbon and some out-of-plane contribution (antibonding) from donor orbitals of the M₂ fragment. Thus, reduction of Cp₂Fe₂(CO)₂(μ-CO)(μ-CSMe)⁺ to a radical would be expected to place an electron in this orbital; if so, delocalization of unpaired electron density onto the sulfur atom might occur. Organic radicals of the type R²C-S-CH₂R' (R' = H, CH₃, C₂H₅) are stabilized by such delocalization of unpaired electron density onto sulfur.^{11,12} EPR spectra

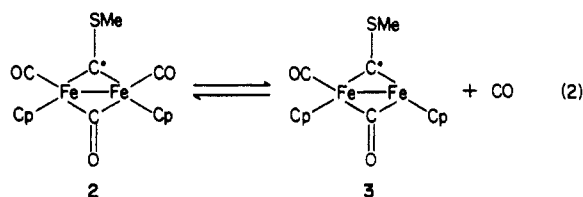
(10) Abrahamson, H. B.; Wrighton, M. S. *Inorg. Chem.* **1978**, *17*, 1003.(11) Russell, G. A. In *Free Radicals*; Kochi, J. K., Ed.; Wiley: New York, 1973; Vol. I, pp 305.(12) McGimpey, W. G.; Depew, M. C.; Wan, J. K. S. *Phosphorus Sulfur* **1984**, *21*, 145.(9) Brown, E. R.; Large, R. F. In *Physical Methods of Chemistry*; Weissberger, A., Rossiter, B. W., Eds.; Wiley: New York, 1971; Part IIA, pp 423–530.

of these organic radicals show hyperfine coupling constants of 1.5–3.25 G with protons on the $\text{CH}_2\text{R}'$ group.^{13,14} Since the EPR signal for $\text{Cp}_2\text{Fe}_2(\text{CO})_2(\mu\text{-CO})(\mu\text{-CSMe})^*$ (**2**) is approximately 10 G wide, coupling to the methyl protons may not be detectable. However, the absence of hyperfine coupling and the broadness of the signal suggest that delocalization of electron density from the carbyne carbon onto the metal fragment is more important than delocalization onto the SMe group. This is reasonable since the LUMO involved does possess some M_2 -fragment character.

There are few reported EPR spectra of dinuclear radicals related to **2**. The EPR spectrum of $\text{Cp}_2\text{Fe}_2(\text{CO})_2(\mu\text{-SCH}_3)_2^{+*}$ does not exhibit hyperfine coupling.¹⁵ Structural studies of this compound indicate that the unpaired electron resides in an M–M antibonding orbital.^{16,17} Likewise, the radical anions, $\text{R}_2\text{C}_2\text{Co}_2(\text{CO})_6^-$ [$\text{R} = \text{Ph}, \text{Si}(\text{CH}_3)_3, \text{H}, \text{CH}_3, \text{CF}_3, t\text{-Bu}$], show only hyperfine coupling to cobalt.¹⁸ The unpaired electron density in these Co complexes also resides in a predominantly M–M antibonding orbital, as in the case for the $(\text{CH}_3\text{N}(\text{PF}_2)_2)_3\text{Co}_2(\text{CO})_2^{+*}$ radical,¹⁸ as well.

Exchange Reaction of $\text{Cp}_2\text{Fe}_2(\text{CO})_2(\mu\text{-CO})(\mu\text{-CSMe})^*$ (2**) with ^{13}CO .** The chemically generated radical in THF solution undergoes CO exchange when it is stirred under an atmosphere of ^{13}CO for 15 min at 0 °C. The exchanged product was oxidized with I_2 to convert it to the stable carbyne cation, $\text{Cp}_2\text{Fe}_2(\text{CO})_2(\mu\text{-CO})(\mu\text{-CSMe})^+$, which does not undergo CO exchange under these conditions. The IR spectrum of the cation (in CH_3CN) shows $\nu(\text{CO})$ absorptions for the unlabeled cation at 2044 (s) and 1853 (m) cm^{-1} and for the ^{13}CO exchanged cation at 1994 (s) and 1811 (m) cm^{-1} . The positions of the labeled product bands are close to those calculated (1996 and 1811 cm^{-1}) for values of the unlabeled product bands with use of a simple diatomic harmonic oscillator model. The weak CO bands at 2013 cm^{-1} (unlabeled) and 1966 cm^{-1} (labeled) were not resolved in this spectrum. The intensity ratios of the $\nu(\text{CO})$ bands, 2044/1994 and 1853/1811, were approximately 1, indicating that about half of the CO ligands of the radical exchanged in 15 min at 0 °C. The ^1H NMR spectrum of the product of the ^{13}CO exchange and I_2 oxidation showed resonances for $\text{Cp}_2\text{Fe}_2(\text{CO})_2(\mu\text{-CO})(\mu\text{-CSMe})^+$ (**1**) and the ^{13}C NMR spectrum exhibited strongly enhanced bridging (252.0 ppm) and terminal (207.3 ppm) carbonyl resonances for the thiocarbene cation, **1**.

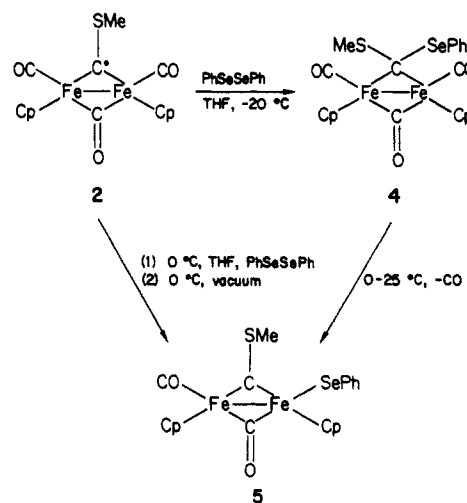
The ^{13}CO exchange studies clearly show that the CO groups in radical **2** are much more labile than those in cation **1**. Although no kinetic studies of this exchange have been undertaken, it is likely that the exchange occurs by rate-determining CO dissociation (eq 4) followed by rapid addition of a ^{13}CO ligand to give the labeled



product. There is no evidence for the CO-dissociated species, **3**, in IR spectra of CH_3CN or THF solutions of **2**, which indicates that equilibrium **2** strongly favors the undissociated radical.

Although equilibrium **2** suggests that a terminal CO group dissociates, the labeled product contains ^{13}CO equally distributed in the terminal and bridging positions. It seems unlikely that the bridging and terminal CO groups undergo dissociative exchange

Scheme I



with ^{13}CO at the same rate; therefore, the terminal and bridging CO ligands in **2** (or possibly **3**) must exchange sites rapidly.

Reaction of $\text{Cp}_2\text{Fe}_2(\text{CO})_2(\mu\text{-CO})(\mu\text{-CSMe})^*$ (2**) with PhSeSePh and PhSSPh .** The chemically generated radical reacts with PhSeSePh at -20 °C to give the purple μ -carbene complex, $\text{Cp}_2\text{Fe}_2(\text{CO})_2(\mu\text{-CO})[\mu\text{-C}(\text{SMe})\text{SePh}]$ (**4**) (Scheme I). This product is unstable, decomposing in solution between 0 and 25 °C to give a 31% yield of the brown-black μ -carbyne, $\text{Cp}_2\text{Fe}_2(\text{SePh})(\text{CO})_2(\mu\text{-CO})(\mu\text{-CSMe})$ (**5**).¹ The same reaction at 0 °C immediately gives a purple-brown reaction mixture which contains both the carbene and carbyne complexes as determined by IR; only the μ -carbyne is obtained upon solvent removal at 0 °C. Since the purple μ -carbene complex, **4**, converts to the μ -carbyne product slowly at 0 °C in the absence of a vacuum,¹ but more rapidly under a vacuum, the original products of the reaction of **2** with PhSeSePh must have been both **4** and **5**. The formation of both products might be explained, by assuming that radical **2** reacts with PhSeSePh to give carbene **4**, whereas the CO-dissociated radical **3** reacts to form the carbyne product, and both reactions occur at 0 °C.

The stoichiometric reaction of **2** with PhSSPh at 0 °C gives a 35% isolated yield of μ -carbyne product $\text{Cp}_2\text{Fe}_2(\text{SPh})(\text{CO})_2(\mu\text{-CO})(\mu\text{-CSMe})$ (**6**).¹ A minor amount of μ -carbene $\text{Cp}_2\text{Fe}_2(\text{CO})_2(\mu\text{-CO})[\mu\text{-C}(\text{SMe})\text{SPh}]$ (**7**) is also produced but not isolated. With excess PhSSPh at 0 °C, approximately equal amounts of **6** and **7** are produced as determined by IR spectra of the product mixture. Since **7** does not convert to **6** at a significant rate below 40 °C,¹ these products may be explained by assuming that PhSSPh reacts with both **2** (to give **7**) and **3** (to give **6**).

While PhSSPh does not react with radical **2** at -20 °C, PhSeSePh gives μ -carbene product $\text{Cp}_2\text{Fe}_2(\text{CO})_2(\mu\text{-CO})[\mu\text{-C}(\text{SMe})\text{SePh}]$ (**4**) at this temperature. The greater reactivity of PhSeSePh as compared with PhSSPh may be attributed to several factors, including the following: (1) the weaker Se–Se bond energy (38 kcal/mol)¹⁹ compared with the S–S bond energy (63 kcal/mol) and (2) attack at the smaller sulfur atom being more sterically hindered. Presumably these reactions occur by attack of radical **2** on the disulfide (or diselenide) with displacement of the PhS^* (or PhSe^*) radical, as observed in reactions of RSSR with organic radicals.²⁰ One might consider another mechanism which involves initial electron transfer from **2** to PhSSPh to give **1** and SPh^- . While **1** and SPh^- do react¹ to form **7**, they do not form **6**. Thus, this electron-transfer mechanism does not account for the observed production of **7** and **6** in the reaction of **2** with PhSSR .

Chemically generated **2** fails to react with CH_3SSCH_3 or $\text{PhCH}_2\text{SSCH}_2\text{Ph}$ at 0 °C; no reaction, except decomposition, of

(13) Krusic, P. J.; Kochi, J. K. *J. Am. Chem. Soc.* **1971**, *93*, 846.

(14) Kawamura, T.; Ushio, M.; Fujimoto, T.; Yonezawa, T. *J. Am. Chem. Soc.* **1971**, *93*, 908.

(15) Dessy, R. E.; Stry, F. E.; King, R. B.; Waldrop, M. *J. Am. Chem. Soc.* **1966**, *88*, 471.

(16) Meyer, T. J. *Prog. Inorg. Chem.* **1975**, *19*, 1.

(17) Connelly, N. G.; Dahl, L. F. *J. Am. Chem. Soc.* **1970**, *92*, 7472.

(18) (a) Peake, B. M.; Rieger, P. H.; Robinson, B. H.; Simpson, J. *J. Am. Chem. Soc.* **1980**, *102*, 156. (b) Babonneau, F.; Henry, M.; King, R. B.; El Murr, N. *Inorg. Chem.* **1985**, *24*, 1946.

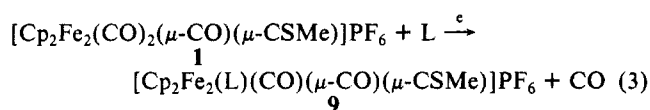
(19) Johnson, D. A. *Some Thermodynamic Aspects of Inorganic Chemistry*; Cambridge Press: London, 1968; pp 158–159.

(20) (a) Hall, D. N.; Oswald, A. A.; Griesbaum, K. *J. Org. Chem.* **1965**, *30*, 3829. (b) Kice, J. L. In *Free Radicals*; Kochi, J. K., Ed.; Wiley: New York, 1973; Vol. II, p 711.

2 occurs on warming the reaction mixture to 25 °C. Relatively stable organic radicals are also less reactive toward dialkyl than diphenyl disulfides,²⁰ which has been attributed to the stronger S–S bonds in dialkyl disulfides compared to diphenyl disulfides.

Redox Reactions of $\text{Cp}_2\text{Fe}_2(\text{CO})_2(\mu\text{-CO})(\mu\text{-CSMe})^+$ (2**).** Addition of stoichiometric amounts of (*t*-BuO)₂ or (PhC(O)O)₂ to chemically generated **2** at 0 °C rapidly gives **1** and *t*-BuO[•] and PhC(O)O[•]. The radical is also rapidly oxidized to **1** by I₂ and [Cp₂Fe]FeCl₄. Electrogenerated **2** reacts instantly with a stoichiometric amount of Co₂(CO)₈ at 0 °C to give cation **1** and Co(CO)₄[•]. Under the same conditions, the reaction of Mn₂(CO)₁₀ and **2** in CH₃CN gives, after 10 min, **1** and Mn(CO)₅[•]. Production of Mn(CO)₅[•] is unexpected since the reverse process, the reaction of Mn(CO)₅[•] and **1** to form Mn₂(CO)₁₀ and **2**, occurs rapidly in THF.⁴ Apparently the NBu₄PF₆ electrolyte and/or THF solvent shifts the equilibrium to favor the formation of the ionic products, **1** and Mn(CO)₅[•], in the reaction of Mn₂(CO)₁₀ with **2**. Organic cations have previously²¹ been observed to affect the stability of organometallic anions in redox reactions. The failure of Re₂(CO)₁₀ to react with **2** under these conditions presumably reflects its much higher reduction potential.²²

Ligand Exchange Reactions of **1 Catalyzed by Electrogenerated **2**.** The substitution of a terminal CO ligand in Cp₂Fe₂(CO)₂(μ-CO)(μ-CSMe)⁺ (**1**) by a phosphorus donor ligand (L) occurs⁵ at room temperature for L = PEt₃ or PMe₂Ph and in refluxing CH₃CN for L = PMePh₂, P(OMe)₃, or CNMe. We find that these reactions proceed rapidly at 0 °C in stirred CH₃CN/0.1 M NBu₄PF₆ solutions when catalyzed by a small cathodic current (eq 3). The conditions of the catalyzed reactions and the results



for L = PEt₃, PMePh₂, PMe₂Ph, PPh₃, or *t*-BuNC

of the studies are given in Table I. A constant 1-mA current was passed through the solution until the potential reached –0.80 V (the reduction potential of **1** is –0.78 V) when the current was stopped; this occurred after 2–3 min except for PPh₃, which had not reacted completely even after 20 min. During the rapid rise to more negative potentials, the color of the reaction solution changed from the brownish-orange of **1** to the yellowish-green of the substituted product. Infrared analysis of the final reaction solution (Table I) showed that all of the ligands, except PPh₃, react completely and cleanly to give the monosubstituted cations. The PPh₃ reaction is only marginally catalytic, giving Cp₂Fe₂(PPh₃)(CO)(μ-CO)(μ-CSMe)⁺, unreacted **1**, and other unknown products probably resulting from the decomposition of **2**. In contrast to the other systems, the PPh₃ reaction solution shows a color change to emerald green during the long electrolysis period, indicating the generation of a high concentration of **2**. The current efficiency of a substitution reaction is given by the ratio of *m*/*n* which is defined as the number of moles (*m*) of **1** consumed per Faraday of charge (*n*) passed through the solution.²³ For all but the PPh₃ reaction, current efficiencies of 30–40 represent significant catalysis of the substitution reaction. The low current efficiency for PPh₃ may be due to the weak Lewis basicity and greater steric requirements of this ligand. It should be noted that there is no reaction between **1** and any of the ligands under the conditions and short times of these reactions when a current is not passed through the solution.

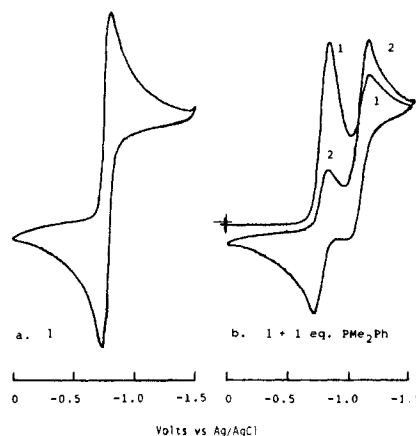
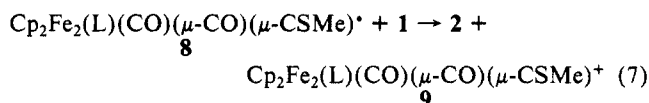
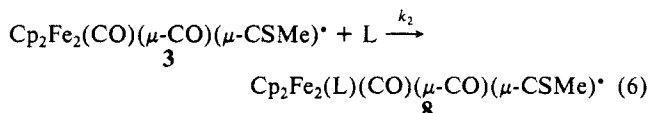
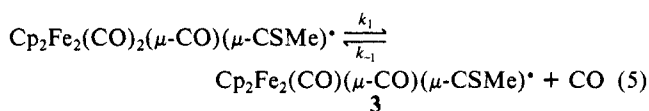
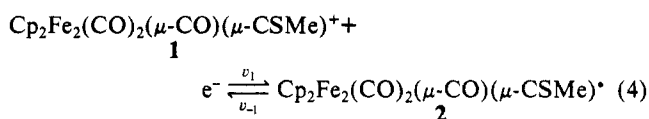


Figure 3. Cyclic voltammograms of **1** (3.0×10^{-2} M) in the absence and presence of PMe₂Ph (3.0×10^{-2} M); scan rate 300 mV/s, CH₃CN (0.1 M NBu₄PF₆), 0 °C.

We suggest the following radical chain mechanism for the overall electrocatalysis process (eq 3):



Since the catalyzed reactions occur at potentials where **1** is reduced to radical **2**, it is likely that the radical is produced in the electrolytic step (eq 4) and is involved in the subsequent catalysis. Indeed, when a catalytic amount of **2** (0.08 equiv) prepared by the Na/naphthalene reduction of **1** at 0 °C is added to a THF solution of **1** (1 equiv) and PEt₃ (6 equiv), Cp₂Fe₂(PEt₃)(CO)(μ-CO)(μ-CSMe)⁺ is formed rapidly. The rapid substitution of CO in **2** by phosphorus ligands (L) in steps 5 and 6 of the proposed mechanism is supported by the fast exchange of ¹³CO with CO ligands in **2**. Further evidence for the rapid substitution of CO in **2** is that chemically generated **2** in THF reacts instantly with PEt₃ or PMePh₂ to give what is likely to be radical **8**; however, as expected, this radical is less stable than radical **2** and decomposes quickly. The product-forming step (eq 7) in the mechanism involves an electron transfer from the phosphine-substituted radical, **8**, to **1** to regenerate radical **2**. That this electron transfer is favorable is established by the reduction potentials for **1** (–0.78 V) and the phosphine-substituted cations, **9** (ca. –1.1 V, Table I). Assuming a steady-state concentration of **3**, the rate of product formation can be expressed as

$$\frac{d[\mathbf{9}]}{dt} = \frac{k_1 k_2 [\text{L}][\mathbf{2}]}{k_{-1}[\text{CO}] + k_2[\text{L}]} \quad (8)$$

Cyclic voltammetric studies of **1** in the presence of various ligands support the above mechanism. For the ligands, (PEt₃, PMe₂Ph, PMePh₂, and *t*-BuNC) which give high current efficiencies (Table I) for reaction 3, the CV scan (Figure 3) for PMe₂Ph is typical. As seen in the figure, the CV of a solution with equal concentrations of **1** and PMe₂Ph shows a quasireversible reduction for **1** at –0.78 V along with a quasireversible wave for

(21) (a) Kirk, C. M.; Peahe, B. M.; Robinson, B. H.; Simpson, J. *Aust. J. Chem.* **1983**, *36*, 441. (b) Darensbourg, M. Y. *Prog. Inorg. Chem.* **1985**, *33*, 221.

(22) Dessy, R. E.; Pohl, R. L.; King, R. B. *J. Am. Chem. Soc.* **1966**, 5121.

(23) Hershberger, J. W.; Amatore, C.; Kochi, J. K. *J. Organomet. Chem.* **1983**, *250*, 345.

the product $\text{Cp}_2\text{Fe}_2(\text{PMe}_2\text{Ph})(\text{CO})(\mu\text{-CO})(\mu\text{-CSMe})^+$ at -1.14 V. On the second cycle the -0.78 -V wave becomes smaller while the -1.14 V wave grows. The voltammogram is essentially unchanged for additional cycles. Thus, the substitution reaction (eq 3) is complete after one cycle. The CV of a stirred solution of **1** and PMe_2Ph shows no anodic waves corresponding to either cathodic peak, indicating that reduced species are not adsorbed to the electrode. The CV of **1** in the presence of 4 equiv of PMe_2Ph is essentially the same as with only 1 equiv. Likewise, the CV of **1** in the presence of 8 equiv of PEt_3 is essentially the same as for PMe_2Ph . This insensitivity of the cyclic voltammograms to the nature and concentration of the phosphine requires the rate of reaction 3 to be independent of the phosphine. This would be true in the mechanism, eq 4–7, if $k_2[\text{L}] \gg k_{-1}[\text{CO}]$; then, the rate law (8) would reduce to $d[\mathbf{9}]/dt = k_1[\mathbf{2}]$, and the rate-determining step would be the dissociation of CO from **2**. This is apparently the case for the ligands (PEt_3 , PMePh_2 , PMe_2Ph , and $t\text{-BuNC}$) that have essentially the same current efficiencies (~ 40 mol/faraday in Table I).

The lower current efficiency for the PPh_3 reaction suggests that $k_2[\text{L}]$ is not larger than $k_{-1}[\text{CO}]$ and that CO competes effectively

with PPh_3 for the coordinatively unsaturated intermediate **3**. In this case, decomposition of **2** would be expected; indeed products of its decomposition are observed.

While detailed kinetic studies of reaction 3 have not been performed, the observed CV's for **1** in the presence of phosphines are similar to computer-simulated CV's²⁴ based on radical chain mechanisms of the type in eq 4–7. Although there have been several recent examples^{23,25} of metal carbonyl substitution reactions which are catalyzed by chemically or electrochemically generated radicals, the present study is the first involving a dinuclear bridging carbyne complex and the first in which the carbyne radical is sufficiently stable to be spectroscopically characterized.

Acknowledgment. We thank the National Science Foundation (Grants CHE-8100419 and CHE-8401844) for support of this research and Dr. D. C. Johnson for helpful discussions.

(24) Feldberg, S. W.; Jestic, L. *J. Phys. Chem.* **1972**, *76*, 2439.

(25) (a) Geiger, W. E.; Connelly, N. G. *Adv. Organomet. Chem.* **1984**, *23*,

1. (b) Geiger, W. E.; Connelly, N. G. *Adv. Organomet. Chem.* **1985**, *24*, 87.

(c) Geiger, W. E. *Prog. Inorg. Chem.* **1985**, *33*, 275.

Preferred Geometry of Cation–Amide Bonding. Crystal Structures of $[\text{Mg}(\text{NMA})_2(\text{H}_2\text{O})_4](\text{NO}_3)_2$ and $\text{Ca}(\text{NO}_3)_2 \cdot 4\text{NMA}$ (NMA = *N*-Methylacetamide)

Krzysztof Lewinski¹ and Lukasz Lebioda^{*2}

Contribution from the Chemistry Department, University of South Carolina, Columbia, South Carolina 29208, and the Chemistry Department, Jagellonian University, ul Karasia 3, Krakow 30-060, Poland. Received November 7, 1985

Abstract: Complexes of *N*-methylacetamide with calcium and magnesium nitrate were studied by X-ray crystallography and IR spectroscopy. Changes in the bond lengths of the amide moiety due to cation–ligand interaction are less than 0.01 Å. A survey of the structures of cation complexes with monodentate, nonbridging amide ligands coordinated through the amide oxygen atom was carried out. It showed that for small cations with M–O distance less than 2.15 Å, there is a preferred geometry of cation–amide binding. It is in the amide plane, trans to the amide N atom and with a M–C=O angle of $135 \pm 15^\circ$. For larger cations the geometry of cation–ligand binding is closer to the direction of the dipole moment of the amide group and in general is less restricted.

Recent interest in the studies of complexes of amides with alkaline-earth cations has been stimulated by the physiological importance of Mg^{2+} and Ca^{2+} and the use of amides like NMA³ as models for polypeptide–cation binding. Peptide carbonyls are frequent ligands in protein– Ca^{2+} complexes⁴ and in some ionophores⁵ and also were implicated in the mechanism of membrane ion pumps.⁶ Complexes of alkali-metal and alkaline-earth cations with amides have been extensively studied by vibrational and NMR spectroscopy, quantum mechanics calculations,⁷ and X-ray crystallography⁸ with the objective being the determination of the

mode of binding, ligand polarization, and the effect of lone electron pairs on the geometry of bonding. It was found that invariably the carbonyl oxygen is the metal coordination site and that polarization of the amide leads to a shift of electron density from the amide N atom to the O atom and the consequently decrease of the double bond character of the C=O bond and an increase of the double bond character of the C–N bond. The degree of polarization varied with ionic radius for both alkali-metal and alkaline-earth cations series, but the relation between those series depends on the method used. Rao and co-workers^{8,9} studied by X-ray crystallography structures of several complexes of alkali-metal and alkaline-earth cations with NMA and DMF and tried to correlate the observed changes between the bond lengths. All their data, however, were of relatively low precision, and in addition anions with weak H-bond accepting properties were used. To verify their hypothesis we have obtained new complexes of NMA with magnesium and calcium nitrate and carried out their structure

(1) Jagellonian University.

(2) University of South Carolina.

(3) Abbreviations used: NMA, *N*-methylacetamide; DMF, *N,N*-dimethylformamide.

(4) Szebenyi, D. M. E.; Obendorf, S. K.; Moffat, K. *Nature (London)* **1981**, *294*, 327–332.

(5) VanRoey, P.; Smith, G. D.; Duax, W. L.; Umen, M. J.; Maryanoff, B. E. *J. Am. Chem. Soc.* **1982**, *104*, 5661–5666.

(6) Urry, D. W.; Trapane, T. L.; Walker, J. T.; Prasad, K. U. *J. Biol. Chem.* **1982**, *257*, 6659–6661.

(7) Over 20 articles on this topic are in: *Metal–Ligand Interactions in Organic Chemistry and Biochemistry*; Pullman, B., Goldblum, N., Eds.; D. Reidel: Dordrecht, 1977.

(8) Chakrabarti, P.; Venkatesan, K.; Rao, C. N. R. *Proc. R. Soc. London, Ser. A* **1981**, *A375*, 127–153.

(9) Pulla Rao, Ch.; Muralikrishna Rao, A.; Rao, C. N. R. *Inorg. Chem.* **1984**, *23*, 1080–1085.